Tennessee Valley Authority Kingston Fossil Plant Harriman, Roane County, Tennessee	**Perimeter Containment** **North Dredge Cell (Dike C) Segment 1** **Sta. A161+50 to A179+50**

Document Control Number	RDP-0113-E
Calculation Package	FPGKIFFESCDX00030020100006

Exhibit 9
Soil Stiffness Properties

Purpose:

- Estimate stiffness and damping properties for ash and soil materials.
- Quantify material parameters needed for 1D ground response analyses and 2D dynamic FLAC analyses.

Methods:

- Available laboratory test data.
- Empirical correlations.
- Typical values for similar materials.

Results:

- Tabulations of material parameters needed for subsequent engineering analyses.

Calculation Performed by: Stantec Consulting Services, Inc.	
Prepared by: YW and AFR, Nov 2010	*Reviewed by:* Multiple reviews of prior drafts
Revisions: 27-Jan-11	

Soil Stiffness Properties

1. Properties for Ground Response Analysis

For the liquefaction analyses, the dynamic loads induced by an earthquake will be predicted using the *ProShake* computer code. This one-dimensional, equivalent linear ground response analysis will simulate the upward propagation of seismic energy using an acceleration time history at the top of hard rock for the design earthquake event(s). The required input data for this analysis includes the ground motion time history, depth to the groundwater table, soil layer thickness, soil unit weight, maximum shear modulus or shear wave velocity of each layer, and damping and modulus reduction relationships.

Shear wave velocity (V_s) in an elastic medium is related to the maximum (small strain) shear modulus (G_{max}):

$$G_{\max} = \rho V_s^2 \qquad 1.1$$

where ρ is the mass density. Values of G_{max} or V_s must be input into *ProShake* for each soil layer; the code will compute values of G_{max} from V_s (or V_s from G_{max}) using Equation 1.1. The values to be used in the ground response analyses are summarized in Table 1.1.

1.1. Maximum Shear Modulus in Embankment Soils

Dynamic test data are not available for the earthen berm, stone aggregates, and the compacted fly ash landfill. To estimate G_{max} for these soils, an empirical correlation proposed by Hardin (1978) was used:

$$\frac{G_{\max}}{P_a} = \frac{625}{0.3 + 0.7e^2} OCR^k \left(\frac{\sigma'_m}{P_a} \right)^{0.5} \qquad 1.2$$

where e is the void ratio and OCR is the overconsolidation ratio. P_a is one atmospheric pressure (101.3 kPa or 2,116 psf) in the same units as G_{max} and the mean effective stress [$\sigma'_m = (\sigma'_1 + \sigma'_2 + \sigma'_3)/3$]. The parameter k is related to plasticity index (PI), and can be interpolated between these values (Hardin and Drnevich 1972):

PI =	0	20	40	60	80	> 100
k =	0.00	0.18	0.30	0.41	0.48	0.50

Assuming K_o conditions and K_o = 0.5, $\sigma'_m = 2\sigma'_v/3$. For the landfilled ash, e = 0.67, PI = 0, and k = 0. Equation 1.2 can then be simplified to:

$$\frac{G_{\max}}{P_a} = 1{,}018 \left(\frac{2\sigma'_v}{3P_a} \right)^{0.5} \qquad 1.3$$

For both the coarse stone and the shot rock, e = 0.64, PI = 0, and k = 0. Then:

$$\frac{G_{\max}}{P_a} = 1{,}065\left(\frac{2\sigma'_v}{3P_a}\right)^{0.5} \qquad 1.4$$

For the earthen berm material, a mid-range value of k = 0.25 (corresponding to PI of about 32) was assumed. The berm will be compacted, so an OCR of 2 is assumed. Then, for e = 0.62, Equation 1.2 simplifies to:

$$\frac{G_{\max}}{P_a} = 1{,}306\left(\frac{2\sigma'_v}{3P_a}\right)^{0.5} \qquad 1.5$$

Expressing G_{max} and σ'_v in units of psf, and substituting P_a = 2,116 psf, the estimates listed in Table 1.1 for the earthen berm, stone aggregates, and the landfilled ash are obtained.

1.2. Shear Wave Velocities in Soil

AECOM measured shear wave velocities at the site in the vicinity of borings 09-103, 09-208, 09-211, and 09-301, using cross-hole seismic testing and/or MASW/MAM (Multi-channel Analysis of Surface Waves/Microtremor Array Measurements). These test results are presented in Exhibit 8. Within a given material, the measured wave velocities increase with depth as a result of the increasing effective stress. Based on this data, shear wave velocities were assigned to the existing hydraulically placed ash, lean clay, and sandy silt to silty sand as summarized in Table 1.1.

Shear wave measurements were also obtained at the project site by Stantec, using the downhole technique in conjunction with cone penetration testing. However, the shear wave arrivals were not well defined in these recorded seismic traces, making it difficult to accurately determine stress wave velocities. The signals recorded by the CPT probe were relatively weak, apparently due to attenuation of the input energy in the soft ash layers, plus weak transmission across interfaces between soft and stiff materials. Better stress wave measurements were obtained from the techniques employed by AECOM, so their data were used to select representative shear wave velocities for each soil.

Because the sensitive silt/clay layer is very thin, a distinct shear wave velocity could not be discerned from the geophysical test data. For the ground response analysis, this thin soil layer was assumed to have the same shear wave velocity as the hydraulically placed ash just above it.

1.3. Shear Wave Velocities in Rock

The available MASW/MAM results did not extend below an elevation of 633 feet. To further characterize the weathered shale, Spectral-Analysis-of-Surface Waves (SASW) tests were performed along nine profiles at the site by the University of Texas at Austin (UT). The UT test results are presented in Exhibit 8. Top of rock was interpreted at elevations of about 670 to 680 feet based on the measured shear wave velocities from six of the nine surveyed profiles. The difference between these interpreted elevations (El. 670 to El. 680) and the top of rock encountered in the borings (El. 700 to El. 714) indicated a zone of moderately to heavily weathered shale with low shear wave velocities.

To develop shear wave velocity profiles in the weathered shale for the ground response analysis, the AECOM MASW/MAM data were used to estimate the shear wave velocities of shales above El. 675, while the UT SASW data were used to estimate the shear wave velocities of shales below El. 675. Three shear wave velocities were assigned to shales above El. 675, depending on their depths below the top of rock. For shales below El. 675, their shear wave velocities (ft/sec) were computed from Equation 1.6.

$$V_s = 10 \cdot D + 2{,}600 \qquad 1.6$$

where D is the depth (feet) below El. 675. The above equation and the UT measured shear wave velocities in shale are shown in Figure 1.1. Based on this equation, the hard rock (V_s = 9,000 ft/sec) was computed at D = 640 feet (El. 35).

1.4. Damping and Modulus Reduction Curves

At shear strains exceeding some small threshold level, soils begin to soften. The softening dynamic response can be represented with shear modulus reduction and damping ratio curves, expressed as functions of the cyclic shear strain (Kramer 1996). Ishibashi and Zhang (1993) developed empirical equations for reduction curves suitable for use in ground response analyses. Based on plasticity index (PI) and mean effective stress (σ'_m), these relationships are available as built-in options within *ProShake* and were selected to model the dynamic behavior of the various soils in the Kingston dredge cell.

Ishibashi and Zhang's (1993) empirical equation for the secant shear modulus (G_{sec}) reduction curve is:

$$\frac{G_{\sec}}{G_{\max}} = K(\gamma, PI) \cdot \left(\sigma'_m\right)^{m(\gamma,PI)-m_0} \qquad 1.7$$

where G_{max} is the small-strain modulus, γ is the cyclic shear strain, PI is the plasticity index, σ'_m is the mean effective stress (in kPa), and:

$$K(\gamma, PI) = 0.5\left\{1 + \tanh\left[\ln\left(\frac{0.000102 + n(PI)}{\gamma}\right)^{0.492}\right]\right\}$$

$$m(\gamma, PI) - m_0 = 0.272\left\{1 - \tanh\left[\ln\left(\frac{0.000556}{\gamma}\right)^{0.4}\right]\right\}\exp\left(-0.0145 PI^{1.3}\right)$$

$$n(PI) = \begin{cases} 0.0 & \text{for } PI = 0 \\ 3.37\times10^{-6} PI^{1.404} & \text{for } 0 < PI \le 15 \\ 7.0\times10^{-7} PI^{1.976} & \text{for } 15 < PI \le 70 \\ 2.7\times10^{-5} PI^{1.115} & \text{for } PI > 70 \end{cases}$$

Ishibashi and Zhang's (1993) empirical equation for the damping ratio (ζ) reduction curve is:

$$\xi = 0.333\left(\frac{1+\exp(-0.0145PI^{1.3})}{2}\right)\left[0.586\left(\frac{G_{\sec}}{G_{\max}}\right)^2 - 1.547\frac{G_{\sec}}{G_{\max}} + 1\right] \qquad 1.8$$

ProShake automatically computes the effective mean pressure, assuming the at-rest earth pressure coefficient (K_o) is 0.5. The lean clay foundation soil has an average *PI* of about 10, the earthen berm is assumed to have *PI* = 32, and the other soils are nonplastic (*PI* = 0). With these properties, both shear modulus reduction and damping ratio curves can then be calculated. Modulus reduction curves computed in this manner for the dredge cell soils, representing the range of *PI* and expected mean effective stress, are plotted in Figure 1.2.

Table 1.1. Shear Wave Velocities or Maximum Shear Moduli

Material Name		γ_t (pcf)	ρ_t (slugs /ft^3)	Depth Increment	V_s (ft/sec)	Maximum Shear Modulus, G_{max} (psf)
Earthen Berm		125	3.89	All	--	$G_{\max} = 60{,}000\sqrt{2\sigma'_v/3}$
Landfilled Ash		109	3.39	All	--	$G_{\max} = 47{,}000\sqrt{2\sigma'_v/3}$
Hydraulically Placed Ash		107	3.33	> El. 770 ft < El. 770 ft	550 720	1.01×10^6 1.72×10^6
Sensitive Silt/Clay		107	3.33	All	720	1.72×10^6
Lean Clay Foundation Soil		130	4.04	All	810	2.65×10^6
Sandy Silt to Silty Sand		128	3.98	All	710	2.01×10^6
Shale	Above El. 675	140	4.35	*below top of rock:* 0-15 ft 15-30 ft >30 ft	1220 1360 1490	6.48×10^6 8.05×10^6 9.66×10^6
	Below El. 675	140	4.35	All	$V_s = 10D + 2{,}600$	$G_{\max} = 4.35 \cdot V_s^2$
Coarse Stone		115	3.57	All	--	$G_{\max} = 49{,}000\sqrt{2\sigma'_v/3}$
Shot Rock		115	3.57	All	--	$G_{\max} = 49{,}000\sqrt{2\sigma'_v/3}$

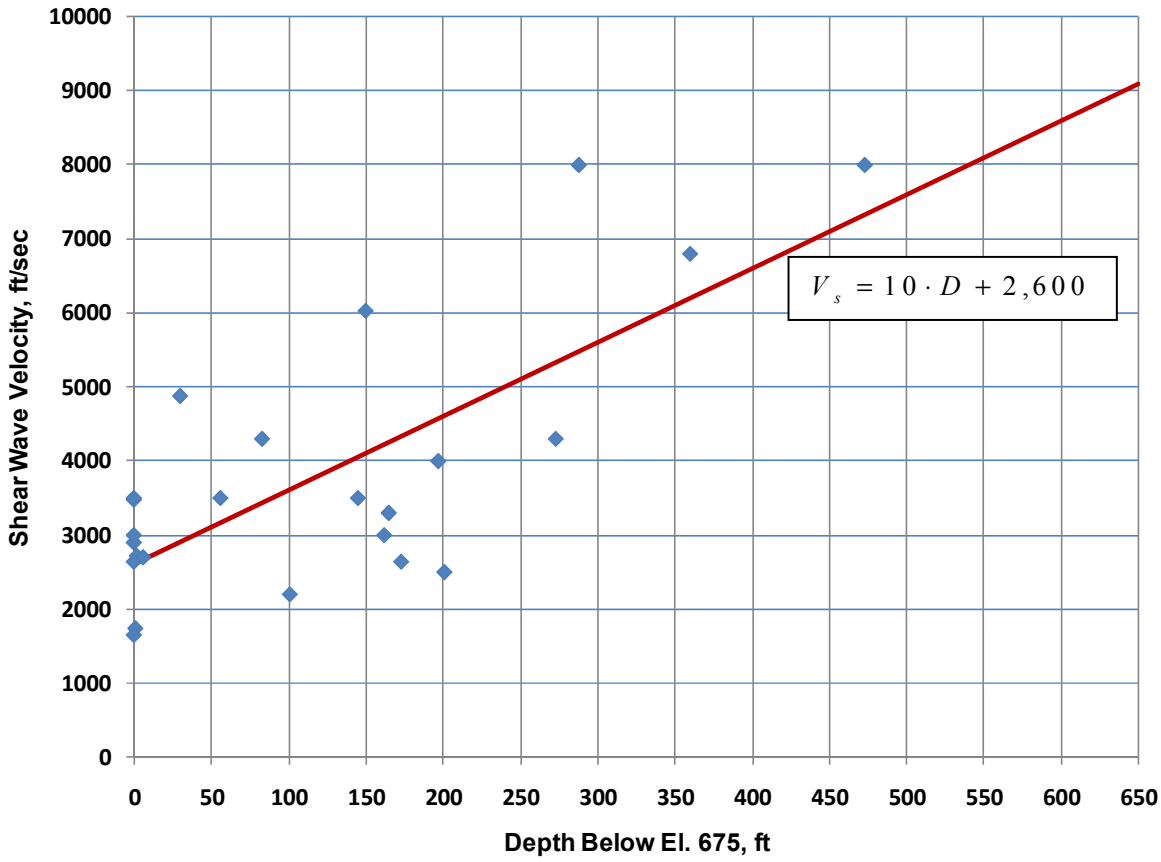

Figure 1.1. Measured Shale Shear Wave Velocity versus Depth below El. 675, and the Trend Line (UT SASW Test Data)

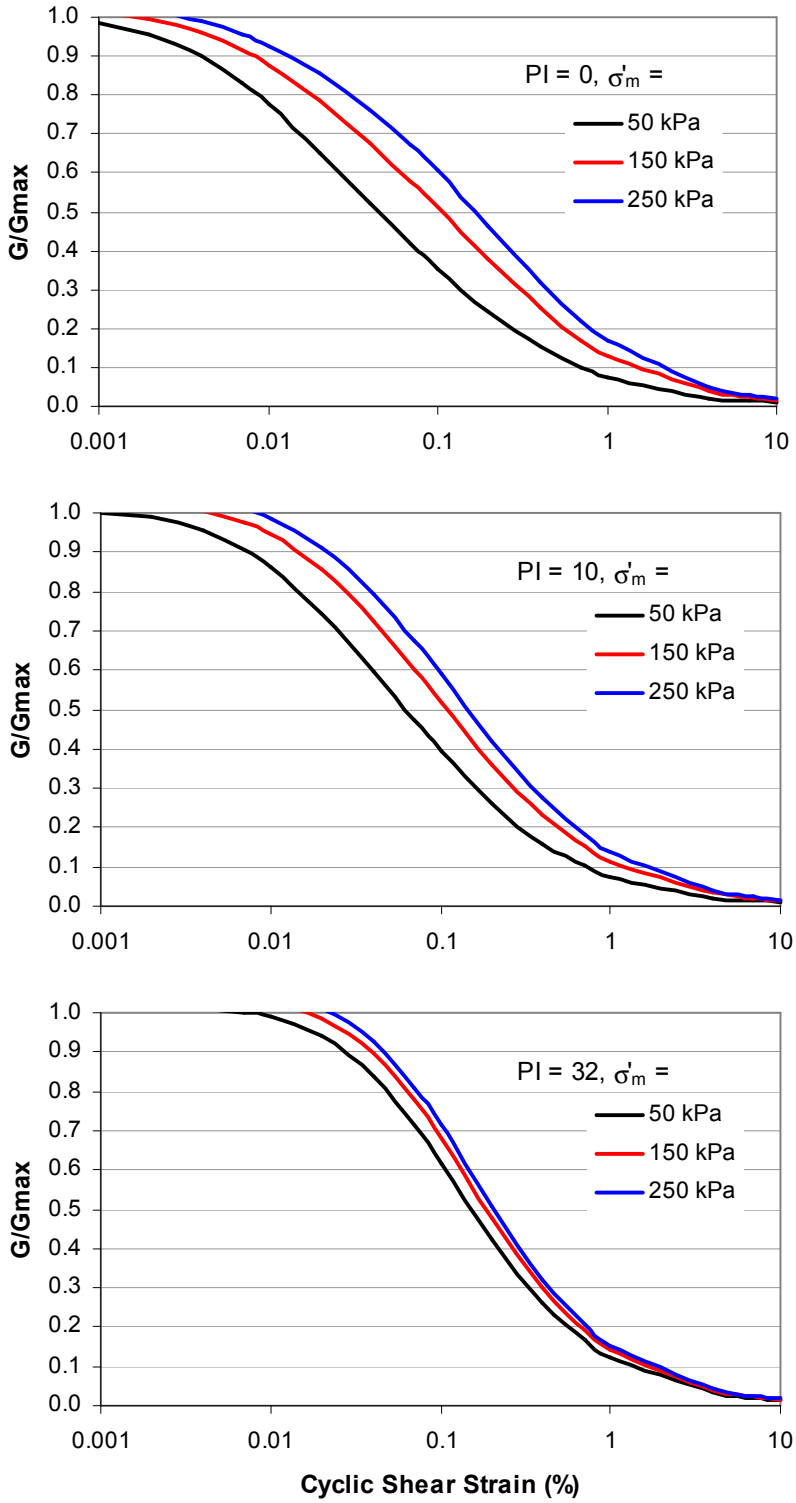

Figure 1.2. Modulus Reduction Curves for the Dredge Cell Soils, Computed using the Empirical Equations from Ishibashi and Zhang (1993)

2. Stiffness for *FLAC* Model

2.1. Characterization of Material Stiffness

The seismic deformation analysis of the closed Kingston dredge cell, with the ash landfill, will be accomplished using the *FLAC* numerical code. The elastic-plastic, Mohr-Coulomb soil model will be used, wherein a linear elastic response is assumed for nonyielding stress states. In *FLAC*, the elastic material response (stiffness) is modeled using the shear modulus (*G*) and bulk modulus (*K*), which must be specified for each soil material in the cross section.

Particulate soils stiffen under higher consolidation pressures and exhibit a nonlinear response; that is, *G* and *K* will increase with higher effective stresses. In the *FLAC* model of the dredge cell, the stiffness stress dependency will be modeled using:

$$G = k_g P_a \left(\sigma'_m / P_a \right)^n \qquad 2.1$$

$$K = k_b P_a \left(\sigma'_m / P_a \right)^m \qquad 2.2$$

Here, σ'_m is the initial mean effective stress [$\sigma'_m = {}^1/_3(\sigma'_1+\sigma'_2+\sigma'_3)$], P_a is one atmosphere of pressure (1 atm = 14.70 psi = 2,116 psf = 101.3 kPa), and k_g, k_b, n, and m are dimensionless coefficients. The form of these equations follows that used by Duncan et al. (1980) and Duncan and Wong (1999).

Stiffness properties were developed to represent two distinct conditions during the *FLAC* simulation of the dredge cell. First, relatively low, constant moduli were selected to represent the soil behavior under long-term, static, drained conditions. The shear response for static conditions was modeled using G_d (Figure 2.1). Higher, strain-dependent moduli were used to represent the stiffer response of the soil under rapid, dynamic loading during a seismic event. The value of G_{max} (Figure 2.1) represents an upper bound on the cyclic shear stiffness at low shear strains. Lower secant stiffness values (G_{sec} in Figure 2.1) were estimated, based on modulus reduction curves, to model the changing dynamic shear response during the earthquake simulation.

The static, drained stiffness parameters (for G_d and K_d) for the Kingston materials were estimated as described in Section 2.2. The needed parameters for the hydraulically placed ash were derived from drained laboratory test data. For all other materials, the drained stiffness parameters were estimated using typical, published values for similar soils. While realistic estimates of G_d and K_d are needed for each material, the accuracy of these estimates will not be critical to the *FLAC* simulation of embankment response during the design earthquake. The drained stiffness will be used only in the static *FLAC* model, where construction of the ash landfill in stages is simulated to obtain reasonable estimates of the stress distribution prior to an earthquake.

Dynamic stiffness parameters were determined for each material based on measured or estimated values of G_{max} (Section 1.1 and Table 1.1). As described in Section 2.3, empirical modulus reduction relationships were then applied to obtain a secant stiffness (G_{sec}) compatible with the magnitude of the computed seismic shear strains. Lacking undrained, dynamic laboratory tests for the site materials, the dynamic stiffness properties could not be

derived from test data. With extensive soil liquefaction predicted, the results from the dynamic *FLAC* simulation will depend on the assigned soil strength parameters, but will be relatively insensitive to the dynamic stiffness properties of each soil. Hence, the method used to estimate G_{sec}, while partially empirical, is acceptable.

The estimation of shear stiffness parameters for the composite, stabilized foundation zones is discussed in Exhibit 14. The bulk moduli of the composite material in these zones, for both static and dynamic loading conditions, were assumed to be unchanged.

2.2. Stiffness Parameters for Static Conditions

To implement the Duncan and Wong (1999) method (Equations 2.1 and 2.2) with the Mohr-Coulomb constitutive model, the bulk and shear modulus were calculated manually for each layer or soil in the *FLAC* static model. The thicknesses of the soil layers in the *FLAC* model were such that the relationship of vertical effective stress to soil modulus was linear over the small range of vertical effective stress in each layer.

2.2.1. Hydraulically Placed Ash

Drained stiffness parameters (k_g, n, k_b, and m, per Equation 2.1 and 2.2) were developed for the hydraulically placed ash using data from five drained triaxial compression tests. Results from these five tests, completed by AECOM using reconstituted samples of ash from the Kingston site, are presented in Exhibit 13. For compression of a triaxial test specimen, the secant Young's modulus (E) is:

$$E = \frac{\Delta\sigma_1}{\varepsilon_a} = \frac{(\sigma_1 - \sigma_3)}{\varepsilon_a} \qquad 2.3$$

where ε_a is the axial strain measured under the applied stress difference, (σ_1-σ_3). The secant bulk modulus (K) at the same point in the triaxial test is:

$$K = \frac{\Delta\sigma_m}{\varepsilon_v} = \frac{\Delta\sigma_1}{3\varepsilon_v} = \frac{(\sigma_1 - \sigma_3)}{3\varepsilon_v} \qquad 2.4$$

where ε_v is the measured volumetric strain. For the ash, secant values of E and K were determined from the five drained tests at 70% of the peak shear stress. This stress level was chosen to represent a typical stiffness for the soil below failure, and is consistent with the recommendations of Duncan et al. (1980) for fitting a nonlinear constitutive model. The shear modulus (G) was then computed from E and K using the elastic equivalency:

$$G = \frac{3KE}{9K - E} \qquad 2.5$$

Values of consolidation pressure (σ_3), G, and K determined from each triaxial test were then normalized with respect to atmospheric pressure (P_a) and plotted using log-log scales (Figure 2.2). The slope and intercept (where σ_3/P_a = 1) of trend lines through these data points represent values of n and k_g (or m and k_b), respectively. The parameters obtained for the hydraulically placed ash are listed in Figure 2.2 and Table 2.3.

2.2.2. Other Materials

Lacking appropriate test data for the other dredge cell soils, drained stiffness parameters were derived from estimates of the constrained moduli and at-rest earth pressure coefficients. First, the tangent constrained modulus (M_d) of each material was estimated based on a relationship suggested by Janbu (1963; 1967; 1985), as summarized by Duncan and Wong (1999):

$$M_d = k_m P_a \left(\sigma'_m / P_a \right)^{0.5} \qquad 2.6$$

where k_m is a dimensionless coefficient and P_a is one atmosphere of pressure in the units of the initial mean effective stress, σ'_m. Values of k_m (Table 2.1) were proposed by Janbu (1963; 1967; 1985) based on studies of foundation settlements. As such, Janbu's constrained moduli represent the stiffness of soils under static, drained conditions. Constrained modulus parameters selected for each material in the Kingston dredge cell are summarized in Table 2.2.

Next, the drained shear and bulk moduli (G_d and K_d) were related to the constrained modulus (M_d) using Poisson's ratio (ν) and these elastic equivalencies:

$$G_d = M_d \frac{1-2\nu}{2(1-\nu)} \qquad 2.7$$

$$K_d = M_d \frac{1+\nu}{3(1-\nu)} \qquad 2.8$$

Substituting Equation 2.6 into Equations 2.7 and 2.8 yields equations matching the form of Equations 2.1 and 2.2. The needed stiffness parameters (Table 2.3) are then $n = m = 0.5$ and:

$$k_g = k_m \frac{1-2\nu}{2(1-\nu)} \qquad 2.9$$

$$k_b = k_m \frac{1+\nu}{3(1-\nu)} \qquad 2.10$$

Poisson's ratio (ν) for each soil was computed from the at-rest lateral earth pressure coefficient (K_0):

$$\nu = \frac{K_o}{1+K_o} \qquad 2.11$$

Values of K_0 were estimated using the correlation suggested by Jaky (1944) for normally consolidated soils:

$$K_o = \frac{\sigma'_h}{\sigma'_v} \approx 1 - \sin\phi' \qquad 2.12$$

Somewhat higher values of K_0 are expected in overconsolidated soils. While the dredge cell soils will be overconsolidated to some degree and are not in an at-rest state, the stress history of each deposit is difficult to quantify and Equations 2.11 and 2.12 were assumed to apply. Estimated values of the drained friction angle for each soil (see Exhibit 13) were then used to estimate the values of K_o and v given in Table 2.3.

2.3. Stiffness Parameters for Seismic Conditions

The dynamic shear response of a generic soil element, with a static applied shear stress, is depicted in Figure 2.1. Initially, the soil will exhibit a high tangent modulus (G_{max}) at low shear strain levels. At the maximum shear strain amplitude, the response can be approximated with a secant modulus (G_{sec}), which will vary with the cyclic strain level.

The small-strain shear stiffness (G_{max}) of each soil was characterized for the ground response analyses, as outlined in Section 1. Estimated values of G_{max} are summarized in the last column of Table 1.1. For the existing soil deposits, these estimates are based on shear wave velocities measured in situ, and are not expressed as a function of stress level. Similar to the calculation used for the static elastic soil properties, G_{max} was manually calculated for each soil layer based on the initial vertical effective stress (from the static *FLAC* simulation).

2.3.1. Dynamic Shear Moduli

To simulate strain softening during dynamic loading, the shear modulus of individual soil zones was reduced during the *FLAC* simulation (based on levels of computed shear strain) using modulus reduction curves that are built into the *FLAC* software. The small-strain shear stiffness (G_{max}) was specified for each soil layer and as the soils experienced shear-induced strain, a secant shear modulus was calculated. *FLAC* measures the shear strain in the individual elements at the end of each calculation cycle, and uses that value of shear strain to compute a secant shear modulus for the next cycle of the calculation. The benefit of this approach over a strain compatible shear modulus (as used in *ProShake*) is that some non-linear behavior can be captured. During quiet periods the shear modulus is not artificially reduced as it is when an average secant modulus is used.

Using estimates of G_{max}, the secant modulus was calculated within *FLAC* using the following:

$$G_{\text{sec}} = G_{\text{max}} \times M_s \qquad 2.13$$

where M_s is the modulus reduction factor taken from the reduction curve for a given cyclic strain. The modulus reduction curves were obtained by fitting a curve to the Seed and Idriss (1970) curve used in *SHAKE*. The S-shaped curve can be represented by the following cubic equation with zero slope and high and low strain cutoffs.

$$M_s = s^2(3 - 2s) \qquad 2.14$$

$$s = \frac{L_2 - L}{L_2 - L_1} \qquad 2.15$$

$$L = \log_{10} \gamma \qquad 2.16$$

where M_s is the modulus reduction factor, L_1 is the lower limit of shear strain and L_2 is the upper limit.

Numerical fits have been developed for sand and clay: L_1 = -3.325, L_2 = 0.823 for sand, and L_1 = -3.156, L_2 = 1.904 for clay. The resulting modulus reduction curves, as used in the *FLAC* model, are plotted in Figure 2.3. Corresponding modulus reduction curves from Figure 1.2 are included, for comparison.

2.3.2. Dynamic Bulk Moduli

The elastic bulk modulus (K) was assumed to remain constant throughout the dynamic *FLAC* simulations, and was calculated based on the relationship with Poisson's ratio (ν) and shear modulus (G_{max}):

$$K = \frac{2\,G_{\max}\,(1+\nu)}{3\,(1-2\nu)} \qquad 2.17$$

The Poisson's ratio for dynamic loading conditions was estimated for each material as follows. The earthen berm, landfilled ash, coarse stone, and shot rock will be mostly unsaturated; the compressibility of the pore air will result in a Poisson's ratio under dynamic load that will be about the same as for static conditions for these materials (values from Table 2.3).

All other modeled materials will be saturated, for which no elastic volumetric change is expected during an earthquake event. A material that exhibits zero volume change under load has, by definition, a Poisson's ratio of 0.5 and an infinite bulk modulus. In reality, the soils will exhibit some small volumetric straining when loaded dynamically, so a finite bulk modulus with ν < 0.5 is realistic. A rational estimate of Poisson's ratio can be obtained by considering that the bulk modulus of an undrained, saturated soil will not exceed the bulk modulus of water (K_{water} = 2,000 MPa = 42,000 ksf). Considering the values of G_{max} in Table 1.1, the largest value of small-strain shear modulus in the saturated soils at the site is 2,650 ksf. Assuming the maximum value of K = K_{water}, the corresponding Poisson's ratio would be:

$$\nu = \frac{3K-2G}{2\,(3K+G)} = \frac{3\cdot 42{,}000 - 2\cdot 2{,}650}{2\,(3\cdot 42{,}000 + 2{,}650)} = 0.47 \qquad 2.18$$

Hence, the computed soil bulk modulus will be less than the bulk modulus of water throughout the mesh if $\nu \leq 0.47$ is specified. A value of ν = 0.47 was thus assigned for the dynamic, elastic response of all saturated materials. Poisson's ratios and bulk moduli used in the seismic simulations are summarized in Table 2.4.

Table 2.1. Janbu's (1963; 1967; 1985) Coefficients (Equation 2.6) for Estimating the Drained Constrained Modulus

	k_m for Normally Loaded Soils	k_m for Preloaded Soils
Relative Density	**Clean Sands and Gravels**	
30%	80-160	240-500
50%	120-240	350-700
70%	200-240	600-1200
In Situ Water Content	**Clays**	
100%	6-12	60-120
50%	9-18	90-180
30%	15-35	150-350
Porosity	**Silts**	
50%	25-50	120-240
40%	60-120	300-600
30%	100-200	500-1000

Table 2.2. Constrained Modulus Parameters (Equation 2.6) for Static, Drained Conditions

Material Name	k_m	Basis for selection of k_m from Table 2.1
Earthen Berm	350	Preloaded (compacted) clay at water content = 20%
Landfilled Ash	450	Preloaded (compacted) silt at void ratio = 0.67 (porosity = 40%)
Hydraulically Placed Ash	--	*Not estimated, drained stiffness fit to test data*
Sensitive Silt/Clay	50	Normally loaded silt at void ratio = 0.85 (porosity = 46%)
Lean Clay Foundation Soil	40	Normally loaded clay with in situ water content of 21% (saturated with void ratio of 0.58)
Sandy Silt to Silty Sand	80	Normally loaded, silty sand with relative density of 25%, based on correlations (US Navy 1986) at dry unit weight of 104 pcf and ϕ' = 30º
Coarse Stone	600	Preloaded (compacted) gravel at 70% relative density
Shot Rock	600	Preloaded (compacted) gravel at 70% relative density

Table 2.3. Soil Stiffness Parameters (Equations 2.1 and 2.2) for Static, Drained Conditions

Material Name	At-Rest Earth Pressure, K_o	Poisson's Ratio, ν	Drained Shear Modulus, G_d		Drained Bulk Modulus, K_d	
			k_g	n	k_b	m
Earthen Berm	0.53	0.35	82	0.5	240	0.5
Landfilled Ash	0.50	0.33	113	0.5	300	0.5
Hydraulically Placed Ash	0.58	0.37	7	1.2	22	1.0
Sensitive Silt/Clay	0.53	0.35	12	0.5	34	0.5
Lean Clay Foundation Soil	0.47	0.32	11	0.5	26	0.5
Sandy Silt to Silty Sand	0.50	0.33	20	0.5	53	0.5
Coarse Stone	0.38	0.28	185	0.5	354	0.5
Shot Rock	0.38	0.28	185	0.5	354	0.5

Table 2.4. Bulk Moduli for Seismic Loading Conditions

Material Name	Poisson's Ratio, ν	Depth Increment	Undrained Bulk Modulus, K (psf)
Earthen Berm	0.35	All	$K = 180{,}000\sqrt{2\sigma'_v / 3}$
Landfilled Ash	0.33	All	$K = 122{,}000\sqrt{2\sigma'_v / 3}$
Hydraulically Placed Ash	0.47	> El. 770 ft < El. 770 ft	1.65×10^7 2.81×10^7
Sensitive Silt/Clay	0.47	All	2.81×10^7
Lean Clay Foundation Soil	0.47	All	4.33×10^7
Sandy Silt to Silty Sand	0.47	All	3.28×10^7
Coarse Stone	0.28	All	$K = 95{,}000\sqrt{2\sigma'_v / 3}$
Shot Rock	0.28	All	$K = 95{,}000\sqrt{2\sigma'_v / 3}$

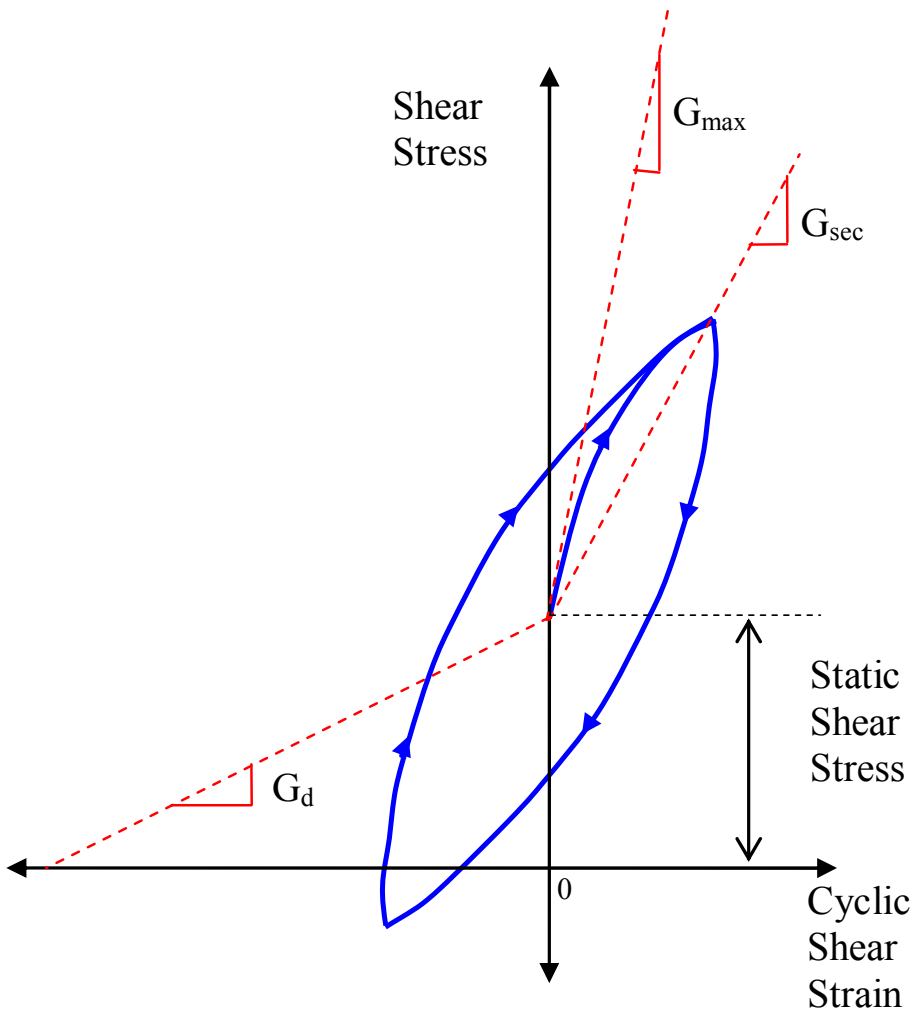

Figure 2.1. Definition of Shear Moduli used to Model Elastic Response for Static and Cyclic Loading

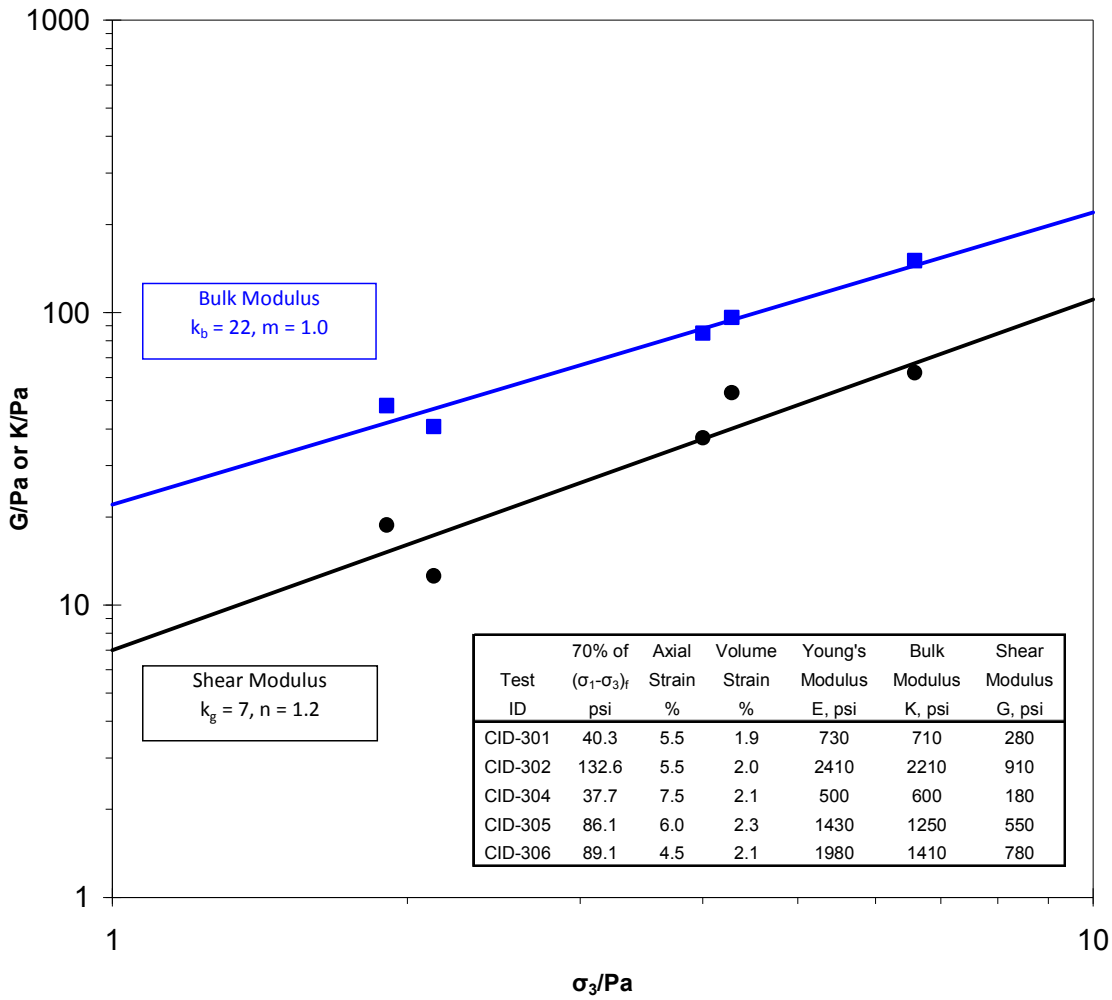

Test ID	70% of $(\sigma_1-\sigma_3)_f$ psi	Axial Strain %	Volume Strain %	Young's Modulus E, psi	Bulk Modulus K, psi	Shear Modulus G, psi
CID-301	40.3	5.5	1.9	730	710	280
CID-302	132.6	5.5	2.0	2410	2210	910
CID-304	37.7	7.5	2.1	500	600	180
CID-305	86.1	6.0	2.3	1430	1250	550
CID-306	89.1	4.5	2.1	1980	1410	780

Figure 2.2. Determination of Drained Stiffness Parameters for Hydraulically Placed Ash using Data from Triaxial Compression Tests Strength for Static Analyses

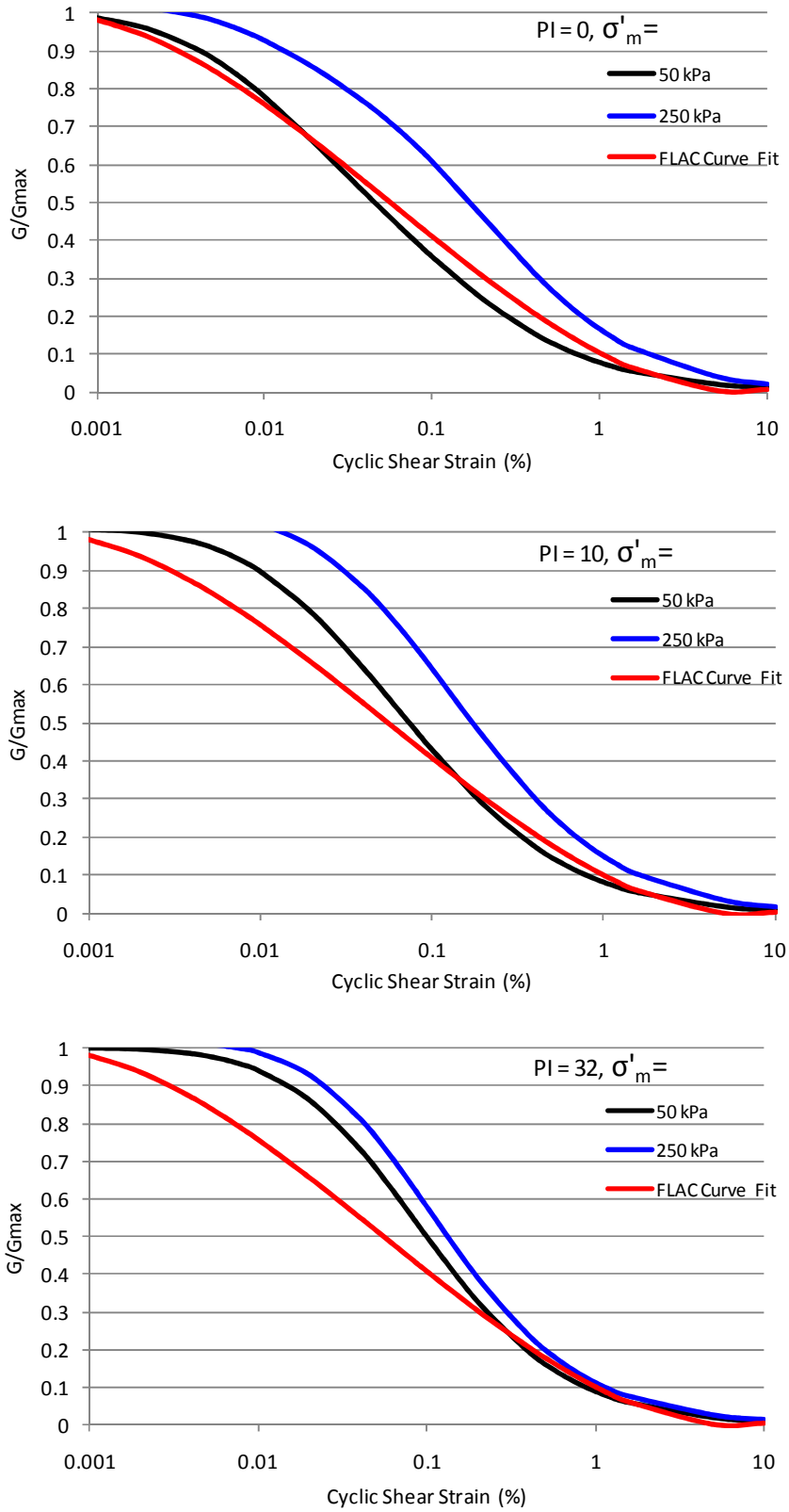

Figure 2.3. Modulus Reduction Curves used in the *FLAC* Model Compared to Empirical Curves from Ishibashi and Zhang (1993)

3. References

Duncan, J. M., Byrne, P., Wong, K. S., and Mabry, P (1980). “Strength, Stress-Strain and Bulk Modulus Parameters for Finite Element Analyses of Stresses and Movements in Soil Masses.” *Report No. UCB/GT/80-01*, College of Engineering, University of California, Berkeley, August.

Duncan, J. M., and Wong, K. S. (1999). “User's Manual for SAGE: Volume II - Soil Properties Manual.” Center for Geotechnical Practice and Research, Dept. of Civil Engineering, Virginia Polytechnic Institute and State University, Blacksburg.

Hardin, B. O. (1978). “The Nature of Stress-Strain Behavior of Soils.” *Proc., Earthquake Engineering and Soil Dynamics,* ASCE, Pasedena, California, Vol. 1, pp. 3-89.

Hardin, B. O., and Drnevich, V. P. (1972). “Shear Modulus and Damping in Soils: Design Equations and Curves.” *J. Soil Mechanics and Foundations Div.,* ASCE, Vol. 98, No. SM7, pp. 667-692.

Ishibashi, I., and Zhang, X. (1993). “Unified Dynamic Shear Moduli and Damping Ratios of Sand and Clay.” *Soils and Foundations*, JSSMFE, Vol. 33, No. 1, pp. 182-191.

Jaky, J. (1944). “The Coefficient of Earth Pressure at Rest.” *J. of the Society of Hungarian Architects and Engineers,* pp. 355-358.

Janbu, N. (1963). "Soil Compressibility as Determined by Odeometer and Triaxial Tests." *Proc., European Conference of Soil Mechanics and Foundation Engineering,* Wiesbaden, Vol. 1, pp. 19-25.

Janbu, N. (1967). "Settlement Calculations Based on Tangent Modulus Concept," *Soil Mechanics and Foundation Engineering Series*, Bulletin No. 2, The Technical University of Norway, Trondheim, 57.

Janbu, N. (1985). "Soil Models in Offshore Engineering," 25th Rankine Lecture, *Géotechnique,* Vol. 35, No. 3, p. 241.

Kramer, S. L. (1996). *Geotechnical Earthquake Engineering.* Prentice Hall, Upper Saddle River, New Jersey.

Seed, H. B., and Idriss, I. (1970). “Soil Moduli and Damping Factors for Dynamic Response Analyses.” Report No. EERC 70-10, Univ. of California at Berkeley

U. S. Navy (1986). “Soil Mechanics.” Design Manual 7.01, Naval Facilities Engineering Command, Alexandria, Virginia.